Active Disturbance Rejection Control for Reference Trajectory Tracking Tasks in the Pendubot System

MARIO RAMÍREZ-NERIA[1], HEBERTT SIRA-RAMÍREZ[2], RUBÉN GARRIDO-MOCTEZUMA[3], ALBERTO LUVIANO-JUÁREZ[4], (Member, IEEE), AND ZHIQIANG GAO[5], (Member, IEEE)

[1]InIAT Instituto de Investigación Aplicada y Tecnología, Universidad Iberoamericana Ciudad de México, Ciudad de Mexico 01219, Mexico
[2]Electrical Engineering Department, Mechatronics Section, Cinvestav-IPN, Mexico City 07360, Mexico
[3]Automatic Control Department, Cinvestav-IPN, Mexico City 07360, Mexico
[4]Instituto Politécnico Nacional–UPIITA, Ciudad de Mexico 07340, Mexico
[5]Department of Electrical and Computer Engineering, Center for Advanced Control Technologies, Cleveland State University, Cleveland, OH 44115, USA

Corresponding author: Alberto Luviano-Juárez (aluvianoj@ipn.mx)

ABSTRACT In this article, an Extended State Observer (ESO) based Active Disturbance Rejection Control (ADRC) scheme is applied to the Pendubot system for a trajectory tracking tasks. The tangent linearization of the system allows to implement the control scheme taking advantage of the differential flatness property, while including a cascade configuration. The proposed method assumes a limited knowledge of the underactuated system where the control input gain and the order of the system are the only needed data. The scheme is experimentally tested leading to accurate tracking results.

INDEX TERMS Active disturbance rejection, Pendubot, underactuated systems, extended state observers, tangent linearization.

I. INTRODUCTION

Up to now, the use of underactuated systems in many engineering applications (spacecraft, aerial robotic systems, underwater vehicles, locomotive systems, flexible robotics, etc) has been increased by virtue of their advantages such as cost reduction, lighter structures, smaller dimensions, among others. However, this class of systems lack of the capacity of being controlled in a wide set of admissible trajectories as in their completely actuated counterpart. Moreover, the main tools of control synthesis such as canonical forms are not general [1], which demand alternative aspects to deal with practical problems as trajectory tracking.

Flatness based control [2]–[4] allows a natural scheme for trajectory tracking control. Even when a wide class of robotic and mechatronic systems satisfies the property [5]–[7], the class of underactuated systems includes several non-differentially flat systems [8]. This fact increases the challenge of developing control laws leading to alternative schemes based on switching controllers [9], [10].

The associate editor coordinating the review of this manuscript and approving it for publication was Hiram Ponce.

Other well-known robust strategies which have been successfully applied are sliding mode control [11], nonlinear control [12], [13], passivity based control [14], etc. In [15], the ball and beam stabilization was tackled through the direct application of the Extended State Observer (ESO) based control, leading to a stability interval. In [16], a gain scheduling ADRC control is designed for a class of underwater vehicles, where the control coefficients are adjusted through a support vector regression. Other schemes implement the ADRC in the context of multiple loop control [17]. Most of these schemes are valid on certain operation intervals, leading to an accurate control tuning task. Besides, the aforementioned strategies are normally used for regulation tasks, and trajectory tracking is still an active area of research.

In [18], it has been shown that the tangent linearization of a class of underactuated systems may lead to a local flat system. Moreover, the tangent linearization lead to a cascade structure where the system can be represented in terms of a tandem set of second order systems connected by physically measurable signals (overcoming a main drawback of flatness-based controllers). This structure allows simple solutions for trajectory tracking in a class of nonlinear underactuated

systems but the locally of the solution needs to be overcome in order to find a suitable practical methodology [19], [20]. Other benefits of the cascade structure allows to enhance the high gain extended state observer based designs through lower gain tuning schemes (see [21])

The increase of the operation region may be taken as a robustness problem, which motivates as alternative the flatness based ADRC control [22]. It consists in obtaining the (flat) tangent linearization of the system which, to be used as a reference model for controlling the actual nonlinear model. The ADRC can equally compensate, both, the nonlinearities neglected in the linearization process as well as the exogenous signals acting as external unknown disturbances. Since the resulting linearized system has the cascade property, the observer order is naturally reduced by using an auxiliary measurable variable, usually in terms of a known position coordinate, instead of a high order time derivative of the flat output. This alternative leads to a simpler observer synthesis with improved results in light of additive noises present in the measured outputs, among other advantages which in practice can solve the problem of trajectory tracking control in this class of underactuated systems. The described control scheme, at least for extended state observers based ADRC methods, has been less explored for underactuated systems, which has encouraged the realization of this study.

In this article, an ESO disturbance observer based ADRC scheme is proposed for the Pendubot in a trajectory tracking task. Concerning the contributions of the article, it is shown that the tangent linearization of the pendubot system satisfies to be flat and having the cascade property, allowing an input-flat output cascade block control design in which the control scheme assumes a simplified model of the Pendubot consisting in a perturbed chain of integrators. The cascade design avoids dealing with complete order controllers, which are substituted by a set of lower order cascade controls that reduce the overshooting effects of high gain designs such as the one ADRC proposal, improving the transient response and improving the trajectory tracking results. This approach allows a control design that stabilizes the vertical equilibrium of the system with large variations of the first link of the robot, which is not common in traditional control approaches of linear and nonlinear class. The control proposal includes a set of extended states which improves the principle of generalized disturbance estimation that is usually stated in terms of a single state. The control scheme is evaluated via an experimental prototype, showing good results in the stabilization error, which is restricted to a small region of the origin. The rest of the article is organized as follows: Section II presents the mathematical model of Pendubot. Section III formulates the problem in terms of a linear output feedback control law using the Extended State Observer based ADRC scheme. Section IV presents the controller and observer design details. The description of a laboratory prototype, as well as the corresponding experimental results are presented in Section V. Finally, a brief discussion of the results and the conclusions are given in Section VI.
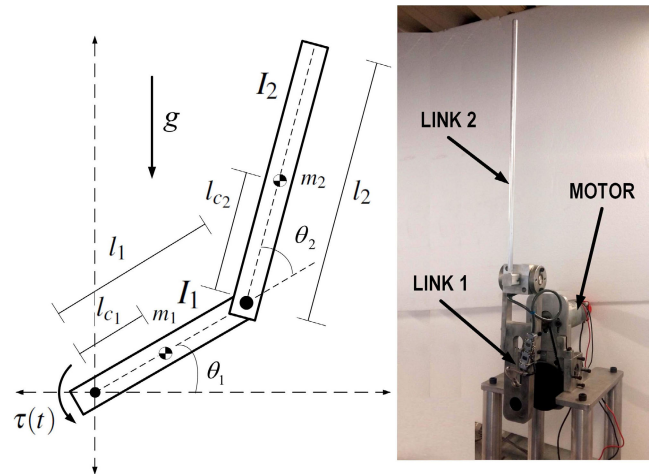

FIGURE 1. Pendubot system schematics and prototype.

II. DYNAMIC MODEL OF PENDUBOT
A. THE NONLINEAR MODEL
The Pendubot is a system consisting of a planar double inverted pendulum as shown in Figure 1, the first link is driven by a DC motor and the second link constitutes an underactuated simple pendulum. The variables θ_1 and θ_2 are the angular positions of the links, and τ_1 represents the control input of the system. The parameters m_1 and m_2 denote the masses, l_1, l_2 represent the lengths of the links, l_{c1} and l_{c2} depict the locations of centers of mass, and I_1 and I_2 denote, respectively, the moments of inertia of the first and the second link, the parameter g being the gravitational constant. The nonlinear model of the mechanical part of the system, was obtained using the Euler-Lagrange formalism [1], [23]. In order to obtain the minimal set of parameters to describe the dynamics of the Pendubot, let define the following constants:

$$\beta_1 = m_1 l_{c1}^2 + m_2 l_1^2 + I_1 \quad \beta_2 = m_2 l_{c2}^2 + I_2$$
$$\beta_3 = m_2 l_1 l_{c2} \quad \beta_4 = m_1 l_{c1} + m_2 l_1$$
$$\beta_5 = m_2 l_{c2}$$

using the above terms, the mathematical model is:

$$M(q)\ddot{q} + C(q,\dot{q})\dot{q} + G(q) = \tau \quad (1)$$

where

$$q = \begin{bmatrix} \theta_1 \\ \theta_2 \end{bmatrix}, \quad \tau = \begin{bmatrix} \tau_1 \\ 0 \end{bmatrix}$$

$$M(q) = \begin{bmatrix} \beta_1 + \beta_2 + 2\beta_3 \cos(\theta_2) & \beta_2 + \beta_3 \cos(\theta_2) \\ \beta_2 + \beta_3 \cos(\theta_2) & \beta_2 \end{bmatrix}$$

$$C(q,\dot{q}) = \begin{bmatrix} -\beta_3 \dot{\theta}_1 \sin(\theta_2) & \beta_3(\dot{\theta}_1 + \dot{\theta}_2)\sin(\theta_2) \\ \beta_3 \dot{\theta}_1 \sin(\theta_2) & 0 \end{bmatrix}$$

$$G(q) = \begin{bmatrix} \beta_4 g \cos(\theta_1) + \beta_5 g \cos(\theta_1 + \theta_2) \\ \beta_5 g \cos(\theta_1 + \theta_2) \end{bmatrix}$$

B. DIFFERENTIAL FLATNESS OF PENDUBOT SYSTEM

Consider the tangent linearization of the dynamics (1) around of the following unstable equilibrium point.

$$\bar{\theta}_1 = \frac{\pi}{2} \quad \bar{\theta}_2 = 0 \ \bar{\tau}_1 = 0 \ \dot{\bar{\theta}}_1 = 0, \ \dot{\bar{\theta}}_2 = 0$$

One readily obtains:

$$(\beta_1 + \beta_2 + 2\beta_3)\ddot{\theta}_{\delta 1} + (\beta_2 + \beta_3)\ddot{\theta}_{\delta 2} - \beta_4 g\theta_1$$
$$- \beta_5 g(\theta_1 + \theta_2) = \tau_1 \quad (2)$$
$$(\beta_2 + \beta_3)\ddot{\theta}_{\delta 1} + \beta_2\ddot{\theta}_{\delta 2} - \beta_5 g(\theta_1 + \theta_2) = 0 \quad (3)$$

where $\theta_{\delta 1} = \theta_1 - \bar{\theta}_1 = \theta_1 - \frac{\pi}{2}$, $\theta_{\delta 2} = \theta_2 - \bar{\theta}_2 = \theta_2$, and $\tau_{\delta 1} = \tau_1 - \bar{\tau}_1 = \tau_1$ are the incremental states. The linearized system (2)-(3) may be expressed in state space representation as,

$$\dot{x}_\delta = Ax_\delta + b\tau_{\delta 1} \quad (4)$$

where A, b and x_δ, as shown at the bottom of the page.

From the Kalman controllability matrix $C_K = \begin{bmatrix} b & Ab & A^2b & A^3b \end{bmatrix}$, the pair (A, B) is controllable since $\det\{C_K\} \neq 0$, it implies that the system (4) is flat, see [22], [24]. The flat output is computed as:

$$f = \begin{bmatrix} 0 & 0 & 0 & 1 \end{bmatrix}\begin{bmatrix} b & Ab & A^2b & A^3b \end{bmatrix}^{-1} x_\delta$$
$$f = \frac{(\beta_2 + \beta_3)\beta_3\beta_5 g}{\beta_2^2(\beta_3^2 - \beta_1\beta_2)}\theta_{1\delta} + \frac{\beta_3\beta_5 g}{\beta_2(\beta_3^2 - \beta_1\beta_2)}\theta_{2\delta} \quad (5)$$

It is not difficult to verify by inspection of (2)-(3) that the flat output can also be chosen as:

$$f_\delta = \frac{\beta_2 + \beta_3}{\beta_2}\theta_{\delta 1} + \theta_{\delta 2} \quad (6)$$

Let recall that, for linear systems, the flat output (5) is unique up a constant factor $f_\delta = \Gamma f$ see [24], thus obtaining (6), where

$$f_\delta = \Gamma \begin{bmatrix} 0 & 0 & 0 & 1 \end{bmatrix}\begin{bmatrix} b & Ab & A^2b & A^3b \end{bmatrix}^{-1} x_\delta \quad (7)$$

and $\Gamma = \frac{\beta_2(\beta_3^2 - \beta_1\beta_2)}{\beta_3\beta_5 g}$ is a constant. The parameter Γ is selected in order to simplify the calculation of the flat output time derivatives. Let us define the row vector

$$c_f = \Gamma \begin{bmatrix} 0 & 0 & 0 & 1 \end{bmatrix}\begin{bmatrix} b & Ab & A^2b & A^3b \end{bmatrix}^{-1} \quad (8)$$

the new flat output f_δ and a finite number of its time derivatives can be obtained using the observability matrix $O_K = \begin{bmatrix} c_f & c_f A & c_f A^2 & c_f A^3 \end{bmatrix}^T$,

$$\begin{bmatrix} f_\delta \\ \dot{f}_\delta \\ \ddot{f}_\delta \\ f_\delta^{(3)} \end{bmatrix} = \begin{bmatrix} c_f \\ c_f A \\ c_f A^2 \\ c_f A^3 \end{bmatrix} x_\delta \quad (9)$$

Computing (9), notice that the flat output (6) and its time derivatives are completely parametrized in terms of the system variables and its time derivatives as:

$$f_\delta = \frac{\beta_2 + \beta_3}{\beta_2}\theta_{\delta 1} + \theta_{\delta 2} \quad (10)$$

$$\dot{f}_\delta = \frac{\beta_2 + \beta_3}{\beta_2}\dot{\theta}_{\delta 1} + \dot{\theta}_{\delta 2} \quad (11)$$

$$\ddot{f}_\delta = \frac{g\beta_5}{\beta_2}(\theta_{\delta 1} + \theta_{\delta 2}) \quad (12)$$

$$f_\delta^{(3)} = \frac{g\beta_5}{\beta_2}(\dot{\theta}_{\delta 1} + \dot{\theta}_{\delta 2}) \quad (13)$$

The relative degree of the system (4) is $n = 4$. The flat output fourth order time derivative is obtained as follows (see [24]).

$$f_\delta^{(4)} = c_f A^3 b\tau_{\delta 1} + c_f A^4 x_\delta$$
$$f_1^{(4)} = \frac{1}{\Gamma}\tau_{\delta 1} + \frac{\beta_4 g}{\Gamma}\theta_{\delta 1} - \frac{\beta_1\beta_5 g}{\beta_3\Gamma}(\theta_{\delta 1} + \theta_{\delta 2}) \quad (14)$$

Note that the second order time derivative of the flat output in (12) can be expressed in terms of angular positions $\theta_{\delta 1}$ and $\theta_{\delta 2}$, this property will be used in the control design procedure in order to estimate the second order time derivative of flat output and higher order derivatives, as a consequence, the added noise to the control law, due to actual measurements, is substantially reduced.

Due to the fact that the flat output is an observable output, all state variables can be parameterized as *differential functions* of the flat output f_δ. This parametrization is computed using the inverse of the observability matrix in (9).

$$\theta_{\delta 1} = \frac{\beta_2}{\beta_3}f_\delta - \frac{\beta_2^2}{\beta_3\beta_5 g}\ddot{f}_\delta \quad (15)$$

$$A = \begin{bmatrix} 0 & 1 & 0 & 0 \\ \frac{(\beta_3\beta_5 - \beta_2\beta_4)g}{\beta_3^2 - \beta_1\beta_2} & 0 & \frac{\beta_3\beta_5 g}{\beta_3^2 - \beta_1\beta_2} & 0 \\ 0 & 0 & 0 & 1 \\ \frac{((\beta_2 + \beta_3)\beta_4 - (\beta_1 + \beta_3)\beta_5)g}{\beta_3^2 - \beta_1\beta_2} & 0 & -\frac{(\beta_1 + \beta_3)\beta_5 g}{\beta_3^2 - \beta_1\beta_2} & 0 \end{bmatrix}$$

$$b = \begin{bmatrix} 0 \\ -\frac{\beta_2}{\beta_3^2 - \beta_1\beta_2} \\ 0 \\ \frac{\beta_2 + \beta_3}{\beta_3^2 - \beta_1\beta_2} \end{bmatrix} \text{ and } x_\delta = \begin{bmatrix} \theta_{\delta 1} & \dot{\theta}_{\delta 1} & \theta_{\delta 2} & \dot{\theta}_{\delta 2} \end{bmatrix}^T.$$

$$\dot{\theta}_{\delta 1} = \frac{\beta_2}{\beta_3}\dot{f}_\delta - \frac{\beta_2^2}{\beta_3\beta_5 g}f_\delta^{(3)} \quad (16)$$

$$\theta_{\delta 2} = \frac{\beta_2(\beta_2 + \beta_3)}{\beta_3\beta_5 g}\ddot{f}_\delta - \frac{\beta_2}{\beta_3}f_\delta \quad (17)$$

$$\dot{\theta}_{\delta 2} = \frac{\beta_2(\beta_2 + \beta_3)}{\beta_3\beta_5 g}f_\delta^{(3)} - \frac{\beta_2}{\beta_3}\dot{f}_\delta \quad (18)$$

$$\tau_{\delta 1} = \Gamma f_\delta^{(4)} + \frac{\beta_2(\beta_1\beta_5 + \beta_2\beta_4)}{\beta_3\beta_5}\ddot{f}_\delta - \frac{\beta_2\beta_4 g}{\beta_3}f_\delta \quad (19)$$

The input-to-flat output relation is obtained using (19) and denoted as:

$$f_\delta^{(4)} = \frac{1}{\Gamma}\tau_{\delta 1} - \frac{(\beta_1\beta_5 + \beta_2\beta_4)g}{(\beta_3^2 - \beta_1\beta_2)}\ddot{f}_\delta + \frac{\beta_4\beta_5 g^2}{(\beta_3^2 - \beta_1\beta_2)}f_\delta \quad (20)$$

As shown in Figure 2, using the second order time derivative of the flat output (12) and the input-to-flat output relation (20), the linearized system can be divided into a cascade connection of 2 blocks: the first one is controlled via the torque input $\tau_{\delta 1}$ whose output is given as the second order time derivative $\ddot{f}$. This output coincides with a linear combination of the pendubot link angular positions, scaled by a constant factor $\ddot{f}_\delta = \frac{g\beta_5}{\beta_2}(\theta_{\delta 1} + \theta_{\delta 2})$. This variable is used as an auxiliary input to the second block, which contains a pure chain of two integrators, where f_δ is the output of the second block and it represents the output of the overall system. The cascade block property simplifies the controller design. Indeed, instead of measuring higher order time derivatives of the flat output that could be substantially affected by non-modeled additive noises, such differentiations are synthesized using measurable angular positions $\theta_{\delta 1}, \theta_{\delta 2}$ and its first order time derivatives, $\dot{\theta}_{\delta 1}$ and $\dot{\theta}_{\delta 2}$.
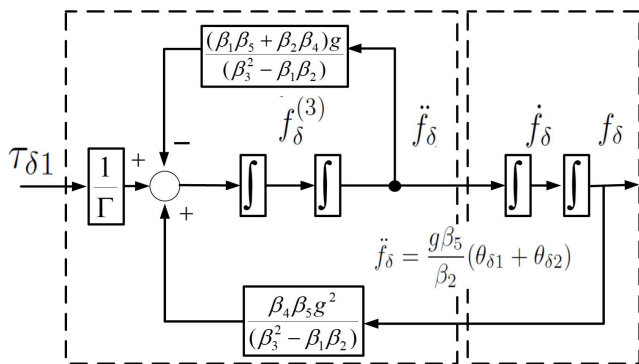

FIGURE 2. Input-flat output cascade block connection.

III. AN ESO BASED ADRC APROACH
A. A LINEAR PERTURBED MODEL REPRESENTATION
In order to apply the Active Disturbance Rejection Controller, and exploiting the flatness property, an additively perturbed chain of integrators representation is necessary. Let us define the trajectory tracking error as:

$$e_{f\delta} = f_\delta - f^*(t) \quad (21)$$

The dynamics of the trajectory tracking error is given by,

$$e_{f\delta}^{(4)} = \frac{1}{\Gamma}(\tau_{\delta 1} - \tau_{\delta 1}^*) - \frac{(\beta_1\beta_5 + \beta_2\beta_4)g}{(\beta_3^2 - \beta_1\beta_2)}\ddot{e}_{f\delta}$$
$$+ \frac{\beta_4\beta_5 g^2}{(\beta_3^2 - \beta_1\beta_2)}e_{f\delta} + H.O.T. \quad (22)$$

where $H.O.T.$ stands for the higher order terms neglected by the linearization. The trajectory tracking error dynamics is represented as a simplified perturbed pure integration system. This is a key step in the flatness based ADRC controller design process:

$$e_{f\delta}^{(4)} = \frac{1}{\Gamma}\tau_{\delta 1} + \psi(t) \quad (23)$$

where $\psi(t)$ is the total disturbance [25], [26] which consists of the effects the neglected internal linear dynamics and the neglected nonlinearities collected in the higher order terms allowing also the possibility of unknown external disturbances.

$$\psi(t) = -\frac{1}{\Gamma}\tau_{\delta 1}^* - \frac{(\beta_1\beta_5 + \beta_2\beta_4)g}{(\beta_3^2 - \beta_1\beta_2)}\ddot{e}_{f\delta}$$
$$+ \frac{\beta_4\beta_5 g^2}{(\beta_3^2 - \beta_1\beta_2)}e_{f\delta} + H.O.T. \quad (24)$$

Define, $e_{f\delta}^{(j)} = e_{fj}$. The trajectory tracking error dynamics (22) is represented in a state space model as follows:

$$\dot{e}_{f0} = e_{f1}$$
$$\dot{e}_{f1} = e_{f2}$$
$$\dot{e}_{f2} = e_{f3}$$
$$\dot{e}_{f3} = \frac{1}{\Gamma}\tau_{\delta 1} + \psi(t) \quad (25)$$

B. A CASCADE ESO
At this point, the cascade property is used by partitioning the state space model of (25) into two subsystems :

$$\dot{e}_{f0} = e_{f1}$$
$$\dot{e}_{f1} = e_{f2} = \frac{g\beta_5}{\beta_2}(\theta_{\delta 1} + \theta_{\delta 2}) - \ddot{f}_\delta^* \quad (26)$$

The perturbation $\psi(t)$ is algebraically observable [27] and represented by time-varying signal $z_1 = \psi(t)$. This disturbance is estimated by a set of six extended states (yielding a fifth order time-polynomial approximation). The second subsystem of (25) may be rewritten as follows:

$$\dot{e}_{f2} = e_{f3}$$
$$\dot{e}_{f3} = \frac{1}{\Gamma}\tau_{\delta 1} + z_1$$
$$\dot{z}_i = z_{i+1}, \quad i = 1, 2, 3, 4, 5$$
$$\dot{z}_6 = 0 \quad (27)$$

As shown in the Figure 3, the cascade property allows us to build a set of two decoupled observers: a Linear Luenberger
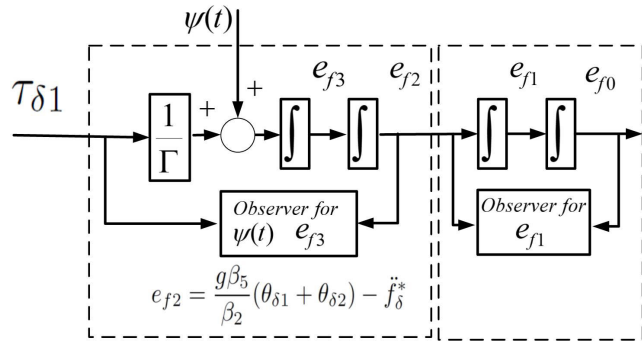
FIGURE 3. Cascade decoupled observer.

observer for (26) and an ESO for (27).

$$\dot{\hat{e}}_{f0} = \hat{e}_{f1} + \gamma_1(e_{f0} - \hat{e}_{f0})$$
$$\dot{\hat{e}}_{f1} = e_{f2} + \gamma_0(e_{f0} - \hat{e}_{f0})$$
$$\dot{\hat{e}}_{f2} = \hat{e}_{f3} + \lambda_7(e_{f2} - \hat{e}_{f2})$$
$$\dot{\hat{e}}_{f3} = \frac{1}{\Gamma}\tau_{\delta1} + \hat{z}_1 + \lambda_6(e_{f2} - \hat{e}_{f2})$$
$$\dot{\hat{z}}_i = \hat{z}_{i+1} + \lambda_{6-i}(e_{f2} - \hat{e}_{f2}), \quad i = 1, 2, 3, 4, 5$$
$$\dot{\hat{z}}_6 = \lambda_0(e_{f2} - \hat{e}_{f2}) \qquad (28)$$

The above decoupled observers simultaneously estimate the phase variables associated with the flat output tracking error $e_{f\delta}$, as well as the total disturbance $\hat{z}_1 = \psi$. The observation error: $\tilde{e}_1 = e_{f0} - \hat{e}_{f0}$, for the incremental flat output tracking error, generates the following linear injected estimation error dynamics:

$$\ddot{\tilde{e}}_0 + \gamma_1\dot{\tilde{e}}_0 + \gamma_0\tilde{e}_0 = 0 \qquad (29)$$

An appropriate choice of the design coefficients $[\gamma_0, \gamma_1]$, places the roots of the corresponding characteristics polynomial deep into the left half of the complex plane. Hence, a second order stable, dominant, characteristic polynomial, may be chosen for the corresponding poles

$$s^2 + \gamma_1 s + \gamma_0 = s^2 + 2\zeta_o\omega_o s + \omega_o^2 \qquad (30)$$

where $\gamma_1 = 2\zeta_o\omega_o$ and $\gamma_0 = \omega_o^2$, for ζ_o, ω_o real positive constants. The tracking error velocity for the flat output $\dot{e}_{f0}$ is, thus, accurately estimated by $\hat{e}_2$ for feedback purposes. The observation error, $\tilde{e}_2 = e_{f2} - \hat{e}_{f2}$, generates the following reconstruction error dynamics:

$$\tilde{e}_2^{(8)} + \lambda_7\tilde{e}_2^{(7)} + \lambda_6\tilde{e}_2^{(6)} \cdots + \lambda_1\dot{\tilde{e}}_2 + \lambda_0\tilde{e}_2 = 0 \qquad (31)$$

Hence, a suitable choice of the design coefficients $\{\lambda_7, \ldots, \lambda_1, \lambda_0\}$ renders an exponentially, decreasing estimation error, $\tilde{e}_2$. Similarly, this result holds for all its time derivatives modulo a small error due to the approximate nature of signal z_1 with respect to the actual total disturbance. The coefficients for the ESO are chosen in accordance with the procedure developed in [28] this methodology for tuning

gains has been successfully applied in [29] and [30]. Consider a characteristic polynomial $p(s)$ of the form:

$$p(s) = a_n s^n + a_{n-1}s^{n-1} + \cdots + a_2 s^2 + a_1 s + a_0,$$
$$a_i > 0, \quad i = 1, 2, \ldots, n \qquad (32)$$

and let α_i be the *characteristic ratios* of $p(s)$. It has been shown [28] that if the following two conditions are satisfied, the polynomial (32) is Hurwitz

$$\text{A) } \alpha_1 > 2; \qquad (33)$$
$$\text{B) } \alpha_k = \frac{\sin\left(\frac{k\pi}{n}\right) + \sin\left(\frac{\pi}{n}\right)}{2\sin\left(\frac{k\pi}{n}\right)}\alpha_1 \qquad (34)$$

for $k = 2, 3, \ldots, n - 1$. The construction of the all-pole stable characteristic polynomial involves only α_1 which we require to be larger than 2. The pole placement procedure is as follows: For an arbitrary positive a_0, and $T > 0$, set,

$$a_1 = Ta_0 \qquad (35)$$
$$a_i = \frac{T^i a_0}{\alpha_{i-1}\alpha_{i-2}^2\alpha_{i-3}^3 \cdots \alpha_1^{i-1}} \quad \text{for } i = 2, 3, \ldots, n \qquad (36)$$

The gains can be chosen as:

$$\lambda_j = \left(\frac{a_j}{a_n}\right) \quad \text{for } j = 0, 1, , 3, \ldots, n - 1 \qquad (37)$$

Thus, the result allows us to characterize the reference all-pole systems by adjusting the parameters α_1 and T to achieve the desired damping.

IV. ADRC CONTROL DESIGN

The control input can be synthesized including an active disturbance canceling strategy for the total disturbance ψ in terms of the estimated $\hat{z}_1$ The output feedback control is given as follows:

$$\tau_{\delta1}(t) = -\Gamma\left[\kappa_3\hat{e}_{f3} + \kappa_2 e_{f2} + \kappa_1\hat{e}_{f1} + \kappa_0 e_{f0} + \hat{z}_1\right] \qquad (38)$$

where, naturally, the tracking errors, e_{f0} and e_{f2}, themselves are used instead of their redundant estimates. Notice that the coefficients of the controller should be chosen in accordance with the fact that, asymptotically, the tracking error is being approximately governed by close-loop differential equation:

$$e_{f0}^{(4)} + \kappa_3 e_{f0}^{(3)} + \kappa_2\ddot{e}_{f0} + \kappa_1\dot{e}_{f0} + \kappa_0 e_{f0} = z_1 - \psi(t) \qquad (39)$$

the set of design coefficients, $[\kappa_0, \kappa_2, \kappa_3, \kappa_4]$, should render the underlying Hurwitz characteristic polynomial

$$s^4 + \kappa_3 s^3 + \kappa_2 s^2 + \kappa_1 s + \kappa_0 = 0 \qquad (40)$$

The control gains were tuned as follows: $\kappa_0 = \omega_c^4$, $\kappa_1 = 4\zeta_c\omega_c^3$, $\kappa_2 = \omega_c^2 + 4\zeta_c^2\omega_c^2$ and $\kappa_4 = 4\zeta_c\omega_c$.
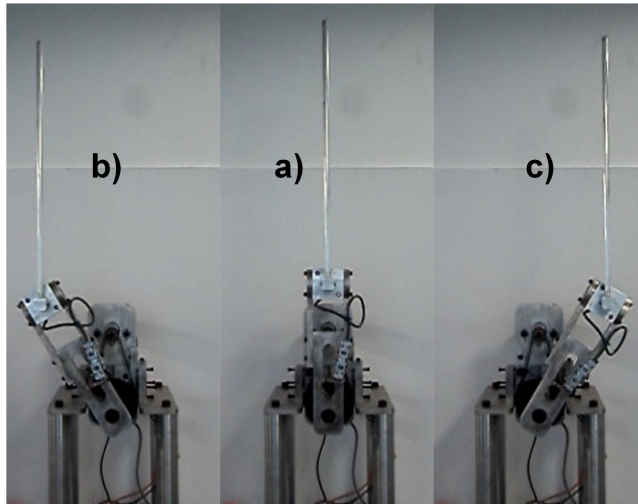
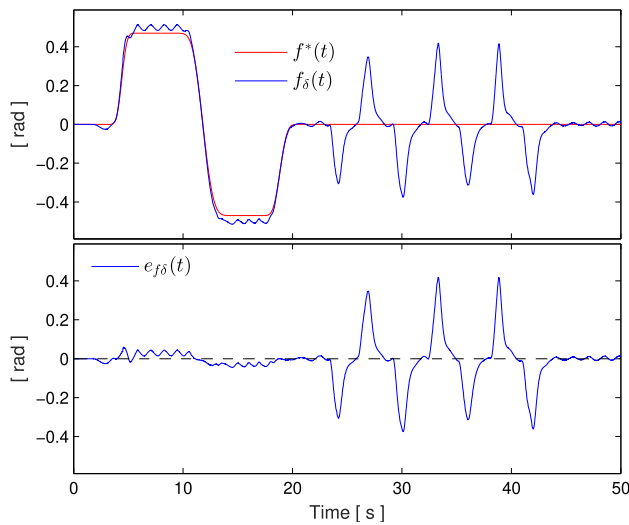**FIGURE 4.** The rest to rest maneuver accomplished by Pendubot system.

FIGURE 6. Link 1 and Link 2 angular position performance.

FIGURE 5. Flat output f_δ closed loop performance.
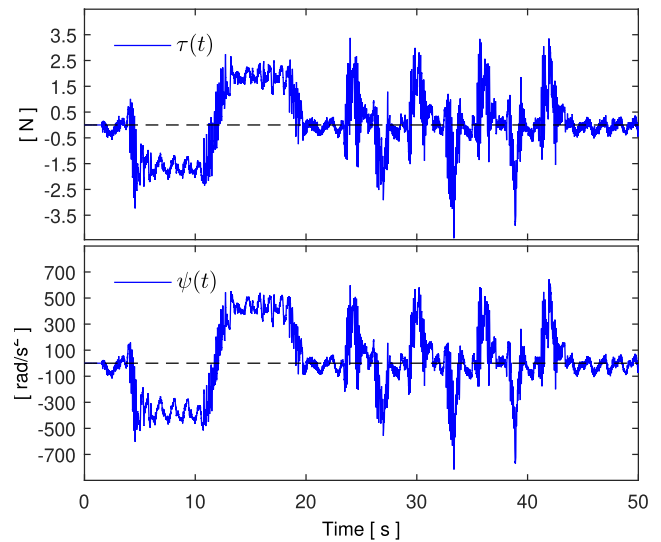
FIGURE 7. Control input torque and lumped on-line disturbance estimation.

V. EXPERIMENTAL RESULTS FOR THE PENDUBOT SYSTEM

Figure 1 shows the experimental Pendubot prototype. It consists of a Brushed servomotor from Moog, model C34L80W40, which drives the link 1 through a synchronous belt with a 4.5:1 ratio. The angles of both links are measured with incremental optical encoders of 2500 Counts Per Revolution. A Copley Controls digital amplifier model Junus 90, working in current mode driving the motor. The Data acquisition is carried out through a data card from Quanser consulting, model QPIDe terminal board. This card reads signals from the optical incremental encoders and supplies control voltages to the power amplifier. The control strategy was implemented in the Matlab-Simulink platform with sampling time set in 0.001[s]. The Pendubot parameters are: Link 1, $I_1 = 0.0481[Kg\text{-}m^2]$, $m_1 = 1.64$ [Kg], $l_1 = 0.33$[m] and Link 2, $I_2 = 0.0036$ [Kg-m^2], $m_2 = 0.141$ [Kg],

$l_2 = 0.55$[m]. The observer gain parameters for the observation error $\tilde{e}_1$ were set to be : $\zeta_o = 2$, $\omega_o = 20$. The observer gain parameters for the observation error $\tilde{e}_2$ were set to be as follows: $n = 8$, $T = 10$, $a_0 = 4$, $\alpha = 4.4$. The controller design parameters were specified to be: $\zeta_c = 0.9$, $\omega_c = 6.3$. The test starts with initial conditions of the joint variables at unstable equilibrium point: $[\theta_1 = \frac{\pi}{2}, \quad \theta_2 = 0]$, this implies that flat output is $f_\delta(0) = 0$ as is shown in Figure 4 a), when the time is $t = 3.5$[s], the flat output move to a rest position shown in Figure 4 b) with $f_\delta(5.5) = \frac{\beta_2 + \beta_3}{\beta_2} \frac{\pi}{5} - \frac{\pi}{5}$ in 2 seconds, it remains in this position 4.5 seconds, when $t = 10.5$ flat output move to a another rest position shown in Figure 4 c) with $f_\delta(13.5) = -\frac{\beta_2 + \beta_3}{\beta_2} \frac{\pi}{5} + \frac{\pi}{5}$ in 2 seconds, it remains in this position 4.5 seconds, finally at $t = 18$[s] returns to initial rest position $f_\delta(20) = 0$ and remains there until the test is finished at $t = 50$[s]. Figure 5 shows the performance of flat

output, ESO based differential flatness allows us carry out tracking trajectories far from the equilibrium point as shown in Figure 4, which states the difference with respect to a simple linear control for the linearized system. The proposed controller acts robustly in spite of the external disturbance forces on Link 2 for $t > 22$[s]. Figure 6 shows Link 1 angular position θ_1, it is moved between a range $[-\frac{\pi}{5}, \frac{\pi}{5}]$[rad] from equilibrium point $\frac{\pi}{2}$[rad], Figure 6 also depicts link 2 angular position θ_2 with similar range between $[-\frac{\pi}{5}, \frac{\pi}{5}]$[rad] from equilibrium point 0[rad]. Control torque input and estimation of total disturbance are depicted in Figure 7, we can notice that the external disturbances forces are estimated on line and canceled effectively with the controller.

In contrast with the classic linear control (state feedback or PID-based controllers [31]), this approach is oriented to provide trajectory tracking solutions which are enhanced by the use of the disturbance observer in combination with the cascade flat structure. Even when the ADRC approach has been successfully applied in underactuated nonlinear systems [15], the control effort and the robustness of the scheme can be enhanced since the order of the observers is reduced by the cascade observer design, which improves the response in presence of noisy measurements.

VI. CONCLUSION AND REMARKS

In this article, the effectiveness of the Extended State Observer based ADRC scheme was experimentally assessed for a rest-to-rest maneuver taking the system far from the unstable equilibrium point used in the linearization of the nonlinear Pendubot system dynamics. The output feedback controller exhibited an excellent behavior in the presence of unknown external disturbances coupled with a lack of a knowledge of the system. An extension of the problem suggested for further study consists in dealing with the problem of simultaneously swinging up and stabilizing the Pendubot within the ESO based ADRC philosophy. The ADRC problem can be enriched if some additional aspects such as quantization effects are addressed [32]. This structure can be focused on a class of mobile robots which satisfy to be underactuated. In this sense, the idea of the cascade property can be used for a more complex problem involving a group of underactuated systems with possible even triggered constraints [33]–[35] which is closely related to Markovian jump systems [36], [37] that can be a wide topic for future investigations.

REFERENCES

[1] R. Olfati-Saber, "Nonlinear control of underactuated mechanical systems with application to robotics and aerospace vehicles," Ph.D. dissertation, Massachussets Inst. Technol., Cambridge, MA, USA, 2000.
[2] M. Fliess, J. Lévine, P. Martin, and P. Rouchon, "Flatness and defect of non-linear systems: Introductory theory and examples," *Int. J. Control*, vol. 61, no. 6, pp. 1327–1361, 1995.
[3] J. Levine, *Analysis and Control of Nonlinear Systems: A Flatness-Based Approach*. Berlin, Germany: Springer, 2009.
[4] J. A. D. Doná, F. Suryawan, M. Seron, and J. Lévine, "A flatness-based iterative method for reference trajectory generation in constrained NMPC," in *Nonlinear Model Predictive Control*. Berlin, Germany: Springer, 2009, pp. 325–333.

[5] Y. Xia, F. Pu, S. Li, and Y. Gao, "Lateral path tracking control of autonomous land vehicle based on ADRC and differential flatness," *IEEE Trans. Ind. Electron.*, vol. 63, no. 5, pp. 3091–3099, May 2016.
[6] Z. Zhang, Y. Wu, and J. Huang, "Differential-flatness-based finite-time anti-swing control of underactuated crane systems," *Nonlinear Dyn*, vol. 87, no. 3, pp. 1749–1761, 2017.
[7] M. Rathinam and R. M. Murray, "Configuration flatness of Lagrangian systems underactuated by one control," *SIAM J. Control Optim.*, vol. 36, no. 1, pp. 164–179, 1998.
[8] H. Sira-Ramírez, E. W. Zurita-Bustamante, and E. Hernández-Flores, "On the ADRC of non-differentially flat, underactuated, nonlinear systems: An experimental case study," in *Proc. 13th ASME/IEEE Int. Conf. Mech. Embedded Syst. Appl.*, vol. 9. Cleveland, OH, USA: American Society of Mechanical Engineers, Aug. 2017, pp. V009T07A014-1–V009T07A014-8.
[9] K. J. Åström and K. Furut, "Swinging up a pendulum by energy control," *Automatica*, vol. 36, no. 2, pp. 287–295, Feb. 2000.
[10] M. W. Spong, "Energy based control of a class of underactuated mechanical systems," *IFAC Proc. Volumes*, vol. 29, no. 1, pp. 2828–2832, Jun. 1996.
[11] R. Xu and Ü. Özgüner, "Sliding mode control of a class of underactuated systems," *Automatica*, vol. 44, no. 1, pp. 233–241, 2008.
[12] M. Reyhanoglu, A. van der Schaft, N. H. McClamroch, and I. Kolmanovsky, "Dynamics and control of a class of underactuated mechanical systems," *IEEE Trans. Autom. Control*, vol. 44, no. 9, pp. 1663–1671, Sep. 1999.
[13] Y. Fang, W. E. Dixon, D. M. Dawson, and E. Zergeroglu, "Nonlinear coupling control laws for an underactuated overhead crane system," *IEEE/ASME Trans. Mechatronics*, vol. 8, no. 3, pp. 418–423, Sep. 2003.
[14] D. Serra, F. Ruggiero, A. Donaire, L. R. Buonocore, V. Lippiello, and B. Siciliano, "Control of nonprehensile planar rolling manipulation: A passivity-based approach," *IEEE Trans. Robot.*, vol. 35, no. 2, pp. 317–329, Apr. 2019.
[15] J. Li, X. Qi, Y. Xia, and Z. Gao, "On asymptotic stability for nonlinear ADRC based control system with application to the ball-beam problem," in *Proc. Amer. Control Conf. (ACC)*, Jul. 2016, pp. 4725–4730.
[16] Z. Yan, Y. Liu, J. Zhou, and D. Wu, "Path following control of an AUV under the current using the SVR-ADRC," *J. Appl. Math.*, vol. 2014, pp. 1–12, Jan. 2014.
[17] W. Chenlu, C. Zengqiang, S. Qinglin, and Z. Qing, "Design of PID and ADRC based quadrotor helicopter control system," in *Proc. Chin. Control Decis. Conf. (CCDC)*, May 2016, pp. 5860–5865.
[18] M. Ramírez-Neria, H. Sira-Ramírez, R. Garrido-Moctezuma, and A. Luviano-Juárez, "Linear active disturbance rejection control of underactuated systems: The case of the Furuta pendulum," *ISA Trans.*, vol. 53, no. 4, pp. 920–928, 2014.
[19] M. Ramírez-Neria, R. Madonski, S. Shao, and Z. Gao, "Robust tracking in underactuated systems using flatness-based ADRC with cascade observers," *J. Dyn. Syst., Meas., Control*, vol. 142, no. 9, p. 9, Sep. 2020.
[20] G. Ochoa-Ortega, R. Villafuerte-Segura, A. Luviano-Juárez, M. Ramírez-Neria, and N. Lozada-Castillo, "Cascade delayed controller design for a class of underactuated systems," *Complexity*, vol. 2020, pp. 1–18, Aug. 2020.
[21] K. Łakomy and R. Madonski, "Cascade extended state observer for active disturbance rejection control applications under measurement noise," *ISA Trans.*, vol. 109, pp. 1–10, Mar. 2021.
[22] H. Sira-Ramirez, A. Luviano-Juárez, M. Ramírez-Neria, and E. W. Zurita-Bustamante, *Active Disturbance Rejection Control of Dynamic Systems: A Flatness Based Approach*. London, U.K.: Butterworth-Heinemann, 2017.
[23] I. Fantoni, R. Lozano, and M. W. Spong, "Energy based control of the pendubot," *IEEE Trans. Autom. Control*, vol. 45, no. 4, pp. 725–729, Apr. 2000.
[24] H. Sira-Ramirez and S. K. Agrawal, *Differentially Flat Systems*. New York, NY, USA: Marcel Dekker, 2004.
[25] J. Han, "From PID to active disturbance rejection control," *IEEE Trans. Ind. Electron.*, vol. 56, no. 3, pp. 900–906, Mar. 2009.
[26] Z. Gao, "Active disturbance rejection control: A paradigm shift in feedback control system design," in *Proc. Amer. Control Conf.*, 2006, p. 7.
[27] S. Diop and M. Fliess, "Nonlinear observability, identifiability, and persistent trajectories," in *Proc. 30th IEEE Conf. Decis. Control*, Dec. 1991, pp. 714–719.

[28] Y. C. Kim, L. H. Keel, and S. P. Bhattacharyya, "Transient response control via characteristic ratio assignment," *IEEE Trans. Autom. Control*, vol. 48, no. 12, pp. 2238–2244, Dec. 2003.

[29] M. Ramirez-Neria, J. L. Garcia-Antonio, H. Sira-Ramirez, M. Velasco-Villa, and R. Castro-Linares, "An active disturbance rejection control of leader-follower Thomson's jumping rings," *Control Theory Appl.*, vol. 30, no. 12, pp. 1564–1572, 2013.

[30] J. Cortés-Romero, G. A. Ramos, and H. Coral-Enriquez, "Generalized proportional integral control for periodic signals under active disturbance rejection approach," *ISA Trans.*, vol. 53, no. 6, pp. 1901–1909, Nov. 2014.

[31] M. Olivares and P. Albertos, "On the linear control of underactuated systems: The flywheel inverted pendulum," in *Proc. 10th IEEE Int. Conf. Control Autom. (ICCA)*, Jun. 2013, pp. 27–32.

[32] S. A. Karthick, R. Sakthivel, Y. K. Ma, S. Mohanapriya, and A. Leelamani, "Disturbance rejection of fractional-order T-S fuzzy neural networks based on quantized dynamic output feedback controller," *Appl. Math. Comput.*, vol. 361, pp. 846–857, Nov. 2019.

[33] Z.-M. Li, X.-H. Chang, and J. H. Park, "Quantized static output feedback fuzzy tracking control for discrete-time nonlinear networked systems with asynchronous event-triggered constraints," *IEEE Trans. Syst., Man, Cybern., Syst.*, vol. 51, no. 6, pp. 3820–3831, Jun. 2021.

[34] J. Sun, J. Yang, S. Li, and W. X. Zheng, "Sampled-data-based event-triggered active disturbance rejection control for disturbed systems in networked environment," *IEEE Trans. Cybern.*, vol. 49, no. 2, pp. 556–566, Feb. 2019.

[35] P. Cheng, S. He, V. Stojanovic, X. Luan, and F. Liu, "Fuzzy fault detection for Markov jump systems with partly accessible hidden information: An event-triggered approach," *IEEE Trans. Cybern.*, early access, Jan. 29, 2021, doi: 10.1109/TCYB.2021.3050209.

[36] P. Cheng, S. He, J. Cheng, X. Luan, and F. Liu, "Asynchronous output feedback control for a class of conic-type nonlinear hidden Markov jump systems within a finite-time interval," *IEEE Trans. Syst., Man, Cybern., Syst.*, early access, Mar. 25, 2020, doi: 10.1109/TSMC.2020.2980312.

[37] P. Cheng, M. Chen, V. Stojanovic, and S. He, "Asynchronous fault detection filtering for piecewise homogenous Markov jump linear systems via a dual hidden Markov model," *Mech. Syst. Signal Process.*, vol. 151, Apr. 2021, Art. no. 107353.

MARIO RAMÍREZ-NERIA received the B.S. degree in mechatronics engineering from the Professional Interdisciplinary Unit of Engineering and Advanced Technologies, National Polytechnic Institute, Mexico City, Mexico, the M.S. degree in electrical engineering from the Mechatronics Section, Electrical Engineering Department, CINVESTAV IPN, and the Ph.D. degree in automatic control from the Automatic Control Department, CINVESTAV-IPN. He is currently with the InIAT Institute of Applied Research and Technology, Universidad Iberoamericana. He is the author of 12 technical articles in refereed journals. He has participated in more than 15 international conferences. He is the coauthor of one book. His current research interests include applications of control theory, active disturbance rejection control, and robotics.

HEBERTT SIRA-RAMÍREZ received the degree in electrical engineering from the Universidad de Los Andes (ULA), Mérida, Venezuela, in 1970, and the M.Sc. degree in electrical engineering and the Ph.D. degree from the Massachusetts Institute of Technology, Cambrdige, MA, USA, in 1974 and 1977, respectively. For 28 years, he worked at ULA, where he retired as a Professor. Since 1998, he has been a Titular Researcher with the Mechatronics Section, Electrical Engineering Department, CINVESTAV-IPN, Mexico City. He is the author of more than 160 technical articles in refereed journals. He has written 31 book chapters and participated in 271 international conferences. He is the coauthor of six books. His research interests include the switched control of nonlinear systems and the control of power electronics systems. He has been involved in the development of algebraic approaches to state and parameter estimation for the control of uncertain systems and active disturbance rejection control.

RUBÉN GARRIDO-MOCTEZUMA received the B.Eng. degree in electrical engineering from the Escuela Superior de Ingeniería Mecánica y Eléctrica—Instituto Politécnico Nacional, Mexico City, Mexico, in 1983, the M.Sc. degree in electrical engineering from the Center for Research and Advanced Studies, National Polytechnic Institute, CINVESTAV-IPN, Mexico City, in 1987, and the Ph.D. degree from the Université de Technology de Compiègne, Compiègne, France, in 1993. He is currently a Professor with the Departamento de Control Automático, CINVESTAV-IPN. His research interests include robot control, parallel robots, visual servoing, parameter identification, electric, pneumatic, hydraulic servomechanisms, adaptive control, and neural network control.

ALBERTO LUVIANO-JUÁREZ (Member, IEEE) received the Ph.D. degree in electrical engineering from the Mechatronics Section, Department of Electrical Engineering, Centro de Investigación y de Estudios Avanzados del Instituto Politécnico Nacional (CINVESTAV-IPN), in 2011. Since then, he has been with the Graduate and Research Section, National Polytechnic Institute (UPIITA). His research interests include robust estimation and control in mechatronic systems, robotics, and algebraic methods in the estimation and control of mechatronic systems.
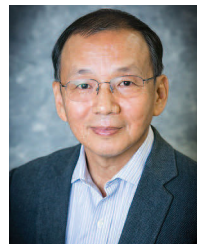
ZHIQIANG GAO (Member, IEEE) received the Ph.D. degree in electrical engineering from the University of Notre Dame, in 1990. He is currently an Associate Professor and the Director of the Center for Advanced Control Technologies, Cleveland State University. His research interests include the principles and practice of engineering cybernetics, particularly its manifestation in active disturbance rejection control.

• • •